Xylan Binding Subsite Mapping in the Xylanase from *Penicillium simplicissimum* Using Xylooligosaccharides as Cryo-Protectant[†,‡]

Andrea Schmidt,[§] Georg M. Gübitz,[||] and Christoph Kratky*[,§]

Institut für Physikalische Chemie, Abteilung für Strukturbiologie, Karl-Franzens Universität Graz, Heinrichstrasse 28, A-8010 Graz, Austria and Institut für Mikrobiologie und Abfalltechnologie, Technische Universität Graz, Petersgasse 12, A-8010 Graz, Austria

Received August 31, 1998; Revised Manuscript Received November 5, 1998

ABSTRACT: Following a recent low-temperature crystal structure analysis of the native xylanase from *Penicillium simplicissimum* [Schmidt et al. (1998) *Protein Sci. 7,* 2081−2088], where an array of glycerol molecules, diffused into the crystal during soaking in a cryoprotectant, was observed within the active-site cleft, we utilized monomeric xylose as well as a variety of linear (Xn, $n = 2$ to 5) and branched xylooligomers at high concentrations (typically 20% w/v) as cryoprotectant for low-temperature crystallographic experiments. Binding of the glycosidic moiety (or its hydrolysis products) to the enzyme's active-site cleft was observed after as little as 30 s soaking of a native enzyme crystal. The use of a substrate or substrate analogue as cryoprotectant therefore suggests itself as a simple and widely applicable alternative to the use of crystallographic flow-cells for substrate-saturation experiments. Short-chain xylooligomers, i.e., xylobiose (X2) and xylotriose (X3), were found to bind to the active-site cleft with its reducing end hydrogen-bonded to the catalytic acid−base catalyst Glu132. Xylotetraose (X4) and -pentaose (X5) had apparently been cleaved during the soaking time into a xylotriose plus a monomeric (X4) or dimeric (X5) sugar. While the trimeric hydrolysis product was always found to bind in the same way as xylotriose, the monomer or dimer yielded only weak and diffuse electron density within the xylan-binding cleft, at the opposite side of the active center. This suggests that the two catalytic residues divide the binding cleft into a "substrate recognition area" (from the active site toward the nonreducing end of a bound xylan chain), with strong and specific xylan binding and a "product release area" with considerably weaker and less specific binding. The size of the substrate recognition area (3−4 subsites for sugar rings) explains enzyme kinetic data, according to which short oligomers (X2 and X3) bind to the enzyme without being hydrolyzed.

Xylanases (EC 3.2.1.8) constitute a group of glycosyl hydrolases, whose biological function—the depolymerization of xylan—can often be exploited in biotechnological applications, such as paper and pulp bleaching procedures. Two main families of xylanases (termed 10 and 11) have been identified on the basis of sequence similarities (*23*, *24*), but substantial structural and functional variablility was found among members of each family, specifically with regard to the mode of depolymerization of the biological substrate. This becomes evident when xylans are treated with a variety of xylanases while changes in physical or chemical properties (degree of depolymerization, liberation of xylo-oligosaccharides) of the reaction mixture are monitored (*18*). Many xylanases also hydrolyze cellulose, though with lower efficiency. An example of such a bifunctional enzyme is the xylanase Cex from *Cellulomonas fimi* (*39*).

Crystal structures of members of both families of xylanases have been determined in recent years [family 10 (*13*, *14*, *19*, *20*, *32*, *41*), family 11 (*9*, *17*, *21*, *37*, *38*)], and the molecular mechanism of hydrolysis of the glycosidic bond is reasonably well understood (*10*, *11*). Accordingly, the most conspicuous feature of the molecular architectures of both types of xylanases is a long groove on the surface of the protein, which acts as the binding site for the xylan chain. A pair of acidic residues (Asp or Glu) from disparate parts of the protein is arranged on opposite sides of this groove and acts as catalytic acid and base, respectively.

While the catalytic action of xylanases is thus well understood in general terms (*10*, *11*), the details of the interactions between the subunits of the glycosidic chain and the protein are less well characterized. It is here, however, where specific aspects of the enzyme function (e.g., endo or exo, minimum size of xylooligomer which is still cleaved, reactivity toward branched substrates, etc.) reside. The number of crystallographic studies of the enzyme−substrate interaction in xylanases (*19*, *22*, *40*) and other glycosyl

[†] This work was supported by the Austrian national science foundation (FWF) through the Spezialforschungsbereich Biokatalyse and through project 11599.

[‡] Crystallographic coordinates have been deposited in the Brookhaven Protein Data Bank (accession numbers 1b3r, 1b3w, 1b3x, 1b3y, 1b3z, 1b30, 1b31).

* To whom correspondence should be addressed. Tel: +43 316 380 5417. Fax: +43 316 380 9850. E-mail Christoph.Kratky@Kfunigraz.ac.at.

[§] Institut für physikalische Chemie.

[||] Institut für Mikrobiologie und Abfalltechnologie.

10.1021/bi982108l CCC: $18.00
Published on Web 02/04/1999

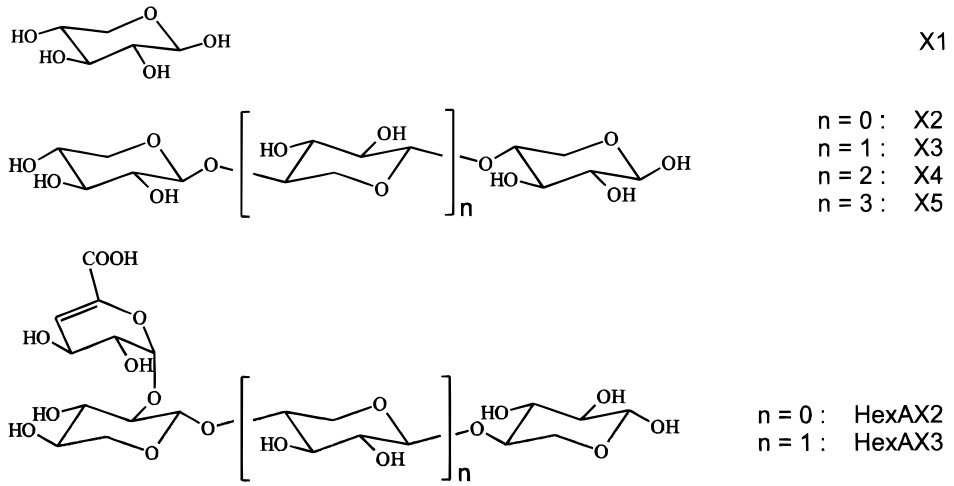

FIGURE 1: Chemical formulas and abbreviations for the xylooligosaccharides used in soaking experiments. (X1) β-D-Xylose. (X2−X5) β-1,4-D-Xylobiose···xylopentaose. (HexAX2, HexAX3) 1,2-(4-Deoxy-β-L-threo-hex-4-enopyranosyluronic acid)-β-1,4-D-xylobiose, ...xylotriose (*36*).

hydrolases (*34*, *35*) has been small. Since native xylooligomer substrates would be rapidly cleaved and released from the enzyme during a typical X-ray experiment, such studies required either a genetic replacement of the catalytic residue(s) (*19*) and/or a chemical modification of the substrate (*22*, *40*) to slow the hydrolysis reaction and trap some intermediate along the reaction path. With such modified enzyme and/or substrate preparations, a typical X-ray experiment then involved either cocrystallization of (mutant) enzyme with substrate (analogues), or soaking of previously produced crystals with (modified) substrate for a relatively long time (typically hours) prior to data collection (*19*, *22*, *40*).

Recently, the crystal structure of the xylanase from *Penicillium simplicissimum* was determined in our laboratory (*32*). This enzyme is an endo-β-1,4-xylanase functioning with overall retention of the anomeric configuration (*16*). It belongs to family 10 of glycosyl hydrolases, displays practically no cellulase activity, and was successfully used for pulp bleaching (*30*). Its crystal structure was determined at cryotemperature (around 100 K). Before cooling, crystals were briefly (several seconds) soaked in a "cryoprotectant" solution with the same composition as the reservoir solution used for crystallization plus about 30% glycerol. Despite the short soaking time, several glycerol molecules were observed in the crystal structure within the active-site groove, at positions suspected to be binding sites for xylose subunits.

Since a variety of substances has in the past been used as cryoprotectants in low-temperature protein crystallography (*15*), including sugars, the above observation suggested the use of a xylooligomer as cryoprotectant for the *P. simplicissimum* xylanase. During soaking of the crystal in a solution with very high glucoside concentration, the active sites of all molecules within the crystal should then be "saturated" with xylooligomer molecules, which are subsequently immobilized by shock-freezing. Crystallographic observation should then yield a similar result as the use of a flow-cell under substrate-saturation conditions, but in a considerably simpler fashion.

Here, we report the results of crystallographic experiments using the substrate as cryoprotectant with a series of xylooligosaccharides (monomer to pentamer, referred to as X1−X5, see Figure 1) in order to investigate the binding of the natural, unmodified substrates to the native enzyme, and to map the xylose subunit binding sites. Moreover, one experiment utilizing a branched substrate [HexAX3, see Figure 1 (*36*)] was performed. To detect substrate-induced conformational changes of the protein, we also redetermined the crystal structure of the native xylanase from *P. simplicissimum* at cryotemperature. Contrary to the previous structure analysis (*32*), we used poly(ethylene glycol) (PEG-200) instead of glycerol as the cryoprotectant (in the following referred to as the "PEG200"-structure): since several glycerol molecules were observed to bind along the active-site cleft (*32*) of crystals cooled in the presence of glycerol (henceforth referred to as the "GLYC"-structure), it was unclear to what extent possible conformational changes might have already been induced. Finally, we also report kinetic parameters for the hydrolysis of di- to hexaxylan by the *P. simplicissimum* xylanase, which we have determined in order to interpret the structural results from these oligomers.

RESULTS

Methodology—Production of Complexes. Complexes between a glycosylhydrolase and oligosaccharides of different lengths can be prepared by soaking a crystal of the enzyme (in our case, of the xylanase from *Penicillium simplicissimum*) in a solution made up from the crystallization broth plus a large amount (typically 20% w/v) of an oligoglucoside. Soaking times are typically 10−30 s, during which time the xylooligomer diffuses into the crystal and interacts with the protein molecules constituting the crystal. After the brief soaking period, the crystal is directly shock-frozen by dumping into liquid nitrogen, and subsequently investigated crystallographically using established cryotemperature protein-crystallographic techniques (*15*). The protein crystal is thus briefly exposed to a saturating concentration of substrate, which simultaneously acts as a cryoprotectant for the freezing step. Contrary to previous experiments aimed at mapping the interaction between glycosyl hydrolases and glycosides (*19*, *22*, *34*, *35*, *40*), the procedure requires neither genetic manipulation of the protein nor chemical modification of the substrate oligomers.

Table 1: Summary of Data Set Statistics and Refinement Results for Data Collected on Xylooligosaccharide Complexes [X1 to HexAX3 (for a Definition See Figure 1)] of the Xylanase from *P. Simplicissimum* and for the Native Xylanase with PEG200 as the Cryoprotectant[a]

substrate	resolution	no. of reflections	R_{merge}	completeness	redundancy	$I/\sigma(I)$ outer shell	no. of atoms	no. of solvent sites	R	*R*(free)	corr (F_oF_c)
X1	15−2.40	17 527	0.185[b]	98.9	5−6	3	2564	220	0.211	0.274	0.901
X2	15−2.60	13 208	0.107	97.4	4−5	2	2535	202	0.199	0.246	0.922
X3	15−2.20	22 429	0.058	98.5	5−6	5	2643	301	0.188	0.240	0.926
X4	15−2.45	16 292	0.116	99.6	4−6	3	2599	254	0.191	0.248	0.926
X5	15−2.30	19 573	0.081	98.8	5−6	5	2711	350	0.180	0.242	0.931
HexAX3	20−2.25	20 885	0.097	99.2	5−6	3	2577	245	0.204	0.261	0.914
PEG200	15−1.70	47 863	0.083	99.8	5−6	3	2659	352	0.213	0.243	0.919

[a] Datasets X1 to HexAX3 were collected inhouse and PEG200 was collected at the EMBL-beamline X11 at DESY in Hamburg (Germany). [b] Crystal twinned.

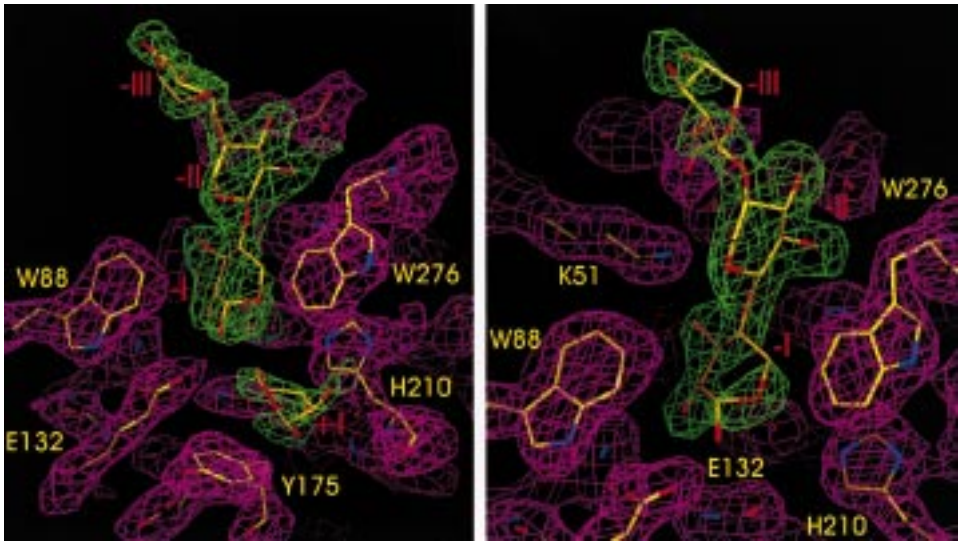

FIGURE 2: Electron density maps ($2F_o - F_c$) of the xylose binding cleft for two soaking experiments. (A, left) 2.45 Å map after soaking with xylotetraose (X4), contoured at 1.3 σ. (B, right) Density after soaking with the branched HexAX3 substrate. Both figures were produced with program O (*25*).

The xylanase from *P. simplicissimum* turned out to be ideally suited for this kind of experiment: its crystals are quite stable, they tolerate (at least for short periods of time) an environment different from that used for crystallization, and therefore, the development of cryocooling conditions was straightforward. Within the crystals, the active site is freely exposed to the solvent and little obstructed by contacts with adjacent molecules.

It is evident that this technique can be adapted for other enzymes, whose substrate(s) can simultaneously act as cryoprotectants, provided a number of conditions are fulfilled: the substrate has to be sufficiently soluble, crystals have to tolerate high substrate concentrations (at least for several seconds) with subsequent flash-cooling, and access to the active site must be unobstructed by crystal contacts.

Structure Determination and Refinement. Crystallographic data sets were collected for the xylooligomer-soaks and for the PEG200 crystals with a maximum resolution between 2.60 and 1.70 A, both inhouse (X1−X5 and HexAX3) and at the EMBL synchrotron radiation facilities in Hamburg, Germany (Peg200). A summary of the data set statistics is given in Table 1. The refinement of the complex structures converged to residuals around 22% or better. Relevant statistics from the refinement are also given in Table 1.

Examples of electron density maps obtained for the X4-as well as the HexAX3-soaks are shown in panels a and b of Figure 2, respectively. The interpretability of the maps differed considerably between different binding subsites, very likely due to disorder and/or incomplete occupancy, as discussed below. Whenever electron density was observed in one of the subsites, it was fitted by a xylose ring in a chair ($^4C_1$) or boat ($4C^1$) conformation.

Description of the Structures. The complex structures are discussed with reference to the established convention (*12*), i.e., xylan monomer binding subsites are numbered negatively (−I, −II, etc.) from the cleavage site (i.e., the location of the two catalytic residues Glu132 and Glu238) toward the nonreducing end of the bound xylan oligomer. Binding subsites in the opposite direction beyond the cleavage site will be denoted by positive roman capitals (+I, +II, etc.). Figure 3 shows a surface representation of the active site cleft, with the superimposed xylooligosaccharides as obtained for the X1−X5 soaks. A schematic representation specifying the assignment of the observed density to the above binding subsites is given in Figure 4.

Xylose (X1-soak). Three molecules of xylose were observed within the active-site cleft, occupying approximately the positions at −II and −III as well as a location intermediate between +I and +II. While the density was well-defined for the molecule in positions −II and still interpretable for the one in −III, the density for the third molecule beyond the cleavage site is considerably less clear. Also, while the molecule in position −II superimposed well with most of the oligomers observed for the other soaks (with the

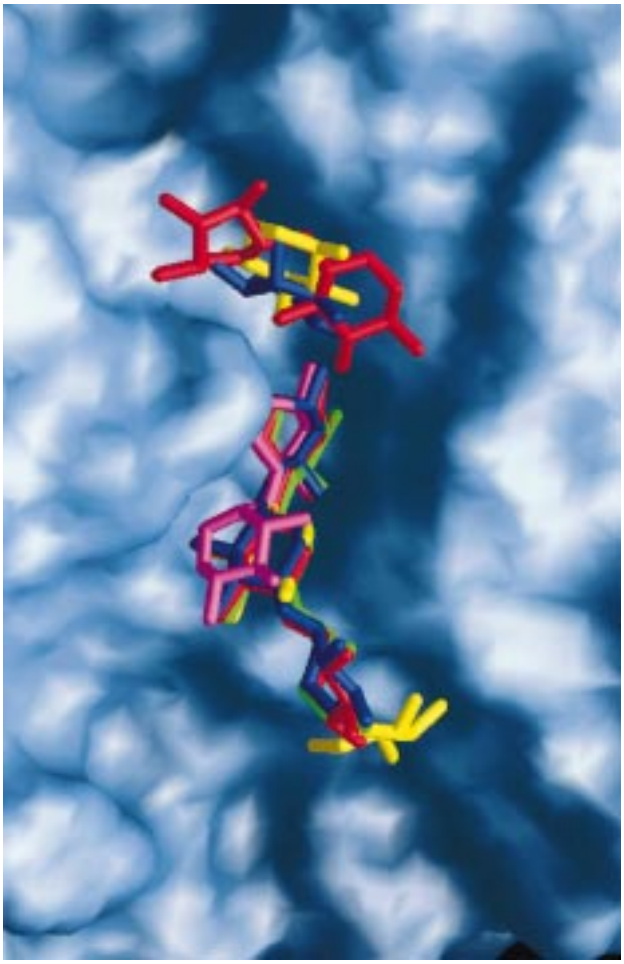

FIGURE 3: Surface representation of the active site cleft of the xylanase from *P. simplicissimum* with bound xylooligosaccharides drawn as capped sticks: X1, yellow; X2, magenta; X3, green; X4, dark blue; and X5, red. Figure produced with program GRASP (28).

exception of X2—see below), the molecule in position −III is somewhat displaced beyond the nonreducing end of the oligomers observed for the X3−X5 soaks. As a consequence of the lack of occupancy of subsite −I, the monomeric xylose does not form a hydrogen bond to the proton donor Glu132, in contrast to all other compounds (see below).

An additional xylose binding subsite outside the xylan binding cleft was observed on the opposite side of the molecule, big enough to hold one xylose monomer by H-bonding contacts to Lys123, Asp68, Asn72, and stacking to Arg119 (see Figure 5b). While this position was also found to be occupied by a well-ordered glycerol molecule in the native GLYC-structure (*32*), some residual but poorly assignable density (possibly originating from water molecules or buffer components) was observed there in all other structures.

Xylobiose (X2-soak). Both rings of the xylobiose molecule were clearly visible in the electron density, occupying positions −I and −II. As in all other oligomers described below, the reducing end oxygen O1 is in H-bonding contact with Glu132, which is proposed to act as the acid−base catalyst (*32*). While the xylan ring occupying subsite −I superimposes very well with the corresponding rings in the X3−X5 structures (see below and Figure 3), the ring on the nonreducing end of the dimer is rotated by 180° around the C1−O1 bond and slightly displaced relative to the orientation found for the corresponding rings in the X3−X5 structures.

Xylotriose (X3-soak). The full xylotriose molecule could be observed in the electron density, with its three xylose rings occupying subsites −I to −III. Again, the reducing end O1 makes a H-bond contact with one of the Glu132 oxygens.

Xylotetraose (X4-soak). The electron density observed for the xylotetraose is shown in Figure 2a. Apparently, the density of the tetrameric species is interrupted at the cleavage site, with three rings occupying subsites −I to −III, as in the X3-soak. The fourth ring appears to be detached from the other three rings, occupying a position intermediate between subsites +I and +II. Its density is less well-defined than the one of the rings in subsites −I to −III.

Xylopentaose (X5-soak). Again, there is no continuous density corresponding to a pentameric xylan chain. Instead, the molecule appears to have been cleaved into xylobiose and xylotriose, the latter occupying subsites −I to −III, very similar to the X3 and X4 structures. The electron density from the dimeric fragment was observed in subsites +I and +II. It is much less clearly defined, permitting only an approximate assignment of the fragment's location and orientation.

The Branched Substrate (HexAX3-soak). Only the "main-chain" xylose rings of the branched compound HexAX3 could be observed in the electron density (subsites −I to −III), as shown in Figure 2b. Compared to the corresponding trimeric moiety in the X3−X5 structures, the electron density from the ring in site −I is weaker, as well as the one from the ring in site −III. Although this ring is slightly disordered, it appears that it is rotated by 180° compared to the corresponding subunit of the other complexes. The hexenuronic acid bound to the xylotriose at its nonreducing end in 2′ position could not be located in the density maps, most probably due to dynamic disorder.

Native Structure with (GLYC) and without (PEG200) Glycerol as Cryoprotectant. The positions of the glycerol molecules observed in the native GLYC-structure (*32*) match the binding sites for the xylose subunits quite well, at least for the molecules in subsites −I and −II. Figure 6b shows a stereoscopic superposition of residues forming the xylan binding cleft, with the glycerol molecules superimposed on the xylooligomer moiety observed in the X4 structure.

Trp 276, which forms a "lid" over the active site was only weakly defined in the native GLYC-structure (*32*) due to apparent rotational freedom of the side chain around the C_β−C_γ bond. With a xylan oligomer in the active-site cleft, the aromatic residue stacks with the xylose ring in the −I subsite, leading to much clearer density. In the PEG200 structure, Trp276 has no xylose ring to interact with, and shows a more "open" conformation with a wider active-site cleft (see Figure 6a). The movement of Trp276 also forces the adjacent Arg277 into a new conformation, and removes the double conformation observed in the native GLYC-structure for the Ser90 hydroxy group on the opposite side of the cleft. Residues at the bottom of the cleft, directly involved in catalysis, appear to be unaffected.

DISCUSSION

Substrate Binding. Family 10 xylanases consist of an elliptical TIM-barrel scaffold, whose top is decorated by

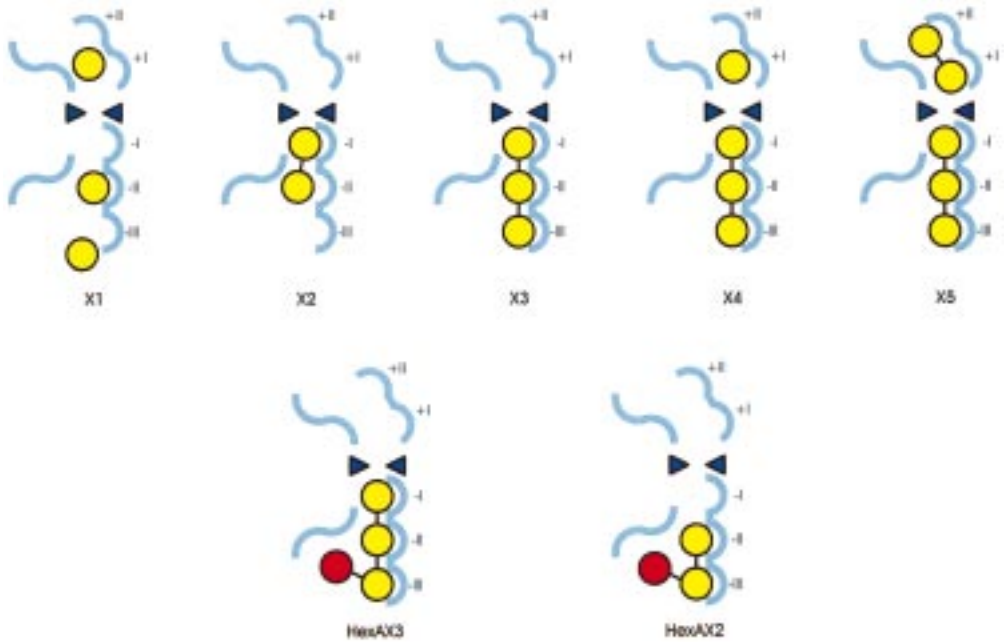

FIGURE 4: Schematic representation of the binding of xylose monomers (X1), oligomers (X2−X5) and of the branched trimer HexAX3 to the xylanase from *P. simplicissimum.*

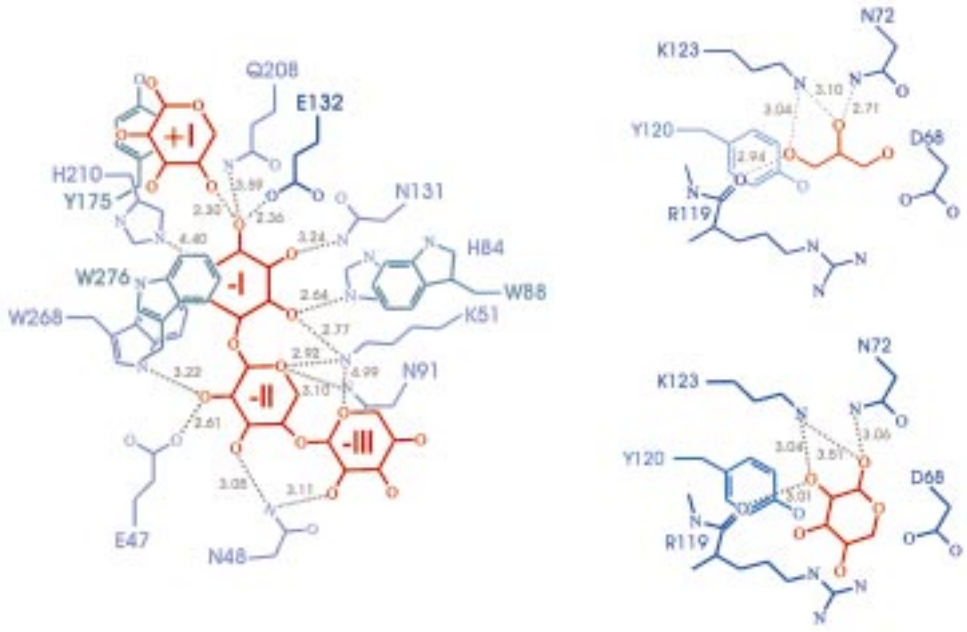

FIGURE 5: (A, left) Schematic representation of the xylose subunit binding sites around the catalytic center in the xylanase from *P. simplicissimum*. Glu132 is the proposed acid−base catalyst during glycosyl hydrolysis. Glu238, the nucleophile (not shown) lies exactly below C1 of the xylose ring in subsite −I. All residues shown are strictly conserved in family 10 xylanases. (B, right) The secondary xylose binding site on the opposite side of the xylanase molecule, as occupied by a glycerol molecule in the native GLYC-structure (top) and by a xylose molecule in xylanase crystals after soaking with xylose (X1, bottom). Tyr120 forms the "bottom" of a shallow depression, but is not in a proper orientation to stack with the incoming sugar ring.

loops arranged to form a long groove extending across the whole of the shorter diameter of the barrel (*32*). The groove is lined by aromatic and hydrophilic residues, and it is generally accepted to constitute the binding site for the substrate xylan polymer. Two catalytic residues, one acting as a nucleophile (Glu238 in the *P. simplicissimum* xylanase) and the other one as an acid−base catalysist (Glu132), protrude into this groove from opposite sides approximately halfway through its length. Crystallographic substrate-diffusion experiments with xylooligomer substrates of 1−5 xylane units under substrate-saturation conditions show smaller oligomers (X2 and X3) to bind to the catalytic groove with their reducing end within hydrogen-bonding distance from the catalytic acid−base catalyst, occupying subsites −I, −II, and (for the triose) −III. Larger oligomers (X4 and X5) appear to have been cleaved between the third and the fourth sugar ring from the nonreducing end. The hydrolysis product comprising the three rings of the nonreducing end is always observed in subsites −I to −III in a conformation very similar to the one of the X3 structure, while the remaining fragment is observed in subsites +I and +II. All xylose rings are structurally complete (i.e., they carry

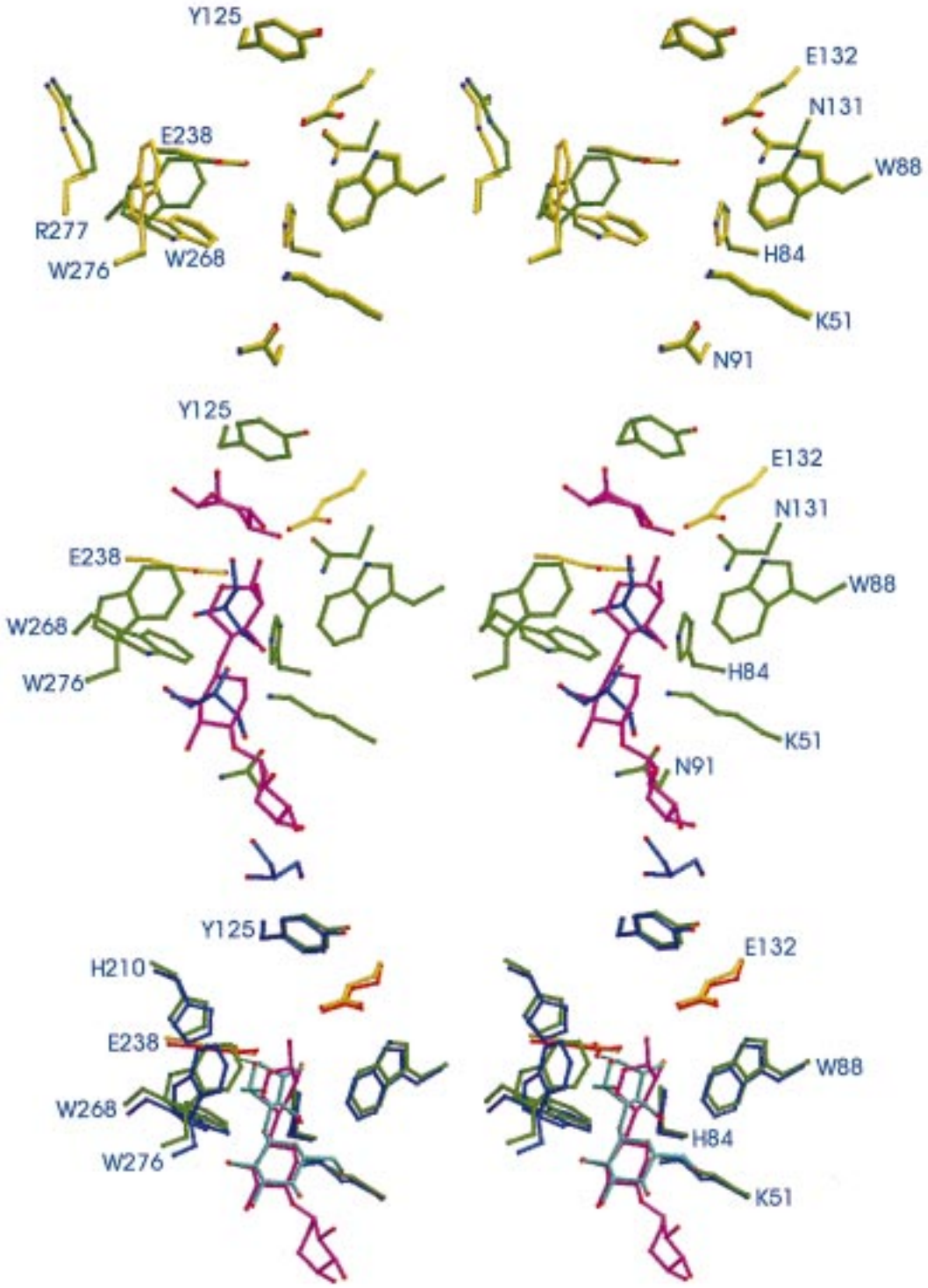

FIGURE 6: Stereo-drawings of the active site cleft of the xylanase from *P. simplicissimum*. (A, top) Environment of Trp276 in the native PEG200 structure (yellow) with the structure of one of the xylooligocomplexes superimposed (green). (B, middle) Result of soaking xylotetraose (X4) into *P. simplicissimum* xylanase crystals (magenta), with the glycerol molecules observed in the native GLYC-structure (*32*) superimposed (blue). The two catalytic residues Glu132 (right) and Glu238 are shown in yellow, other residues interacting with the bound substrate are drawn in green. (C, bottom) Overlay of the active sites residues of the xylanases from *P. simplicissimum* (green/yellow) with bound xylotriose (X3, magenta), superimposed with the *Cellulomonas fimi* xylanase (blue/red) with a covalently attached 2-deoxy-2-fluoro-cellobioside (cyan) (*40*). All figures were drawn with program MOLSCRIPT (*26*).

all their OH groups), indicating that the crystals contain the situation after hydrolysis, with the products already recovered but prior to their release. The ring of the xylose subunit in position −I (bound to Glu132) appears to be less puckered than the other rings, but its anomeric carbon atom C1 is too far away from the nucleophile Glu238 to indicate any interaction.

Interpretation of the results of these experiments naturally divides the substrate-binding cleft into two halves separated by the site of catalytic cleavage, i.e., into an area consisting

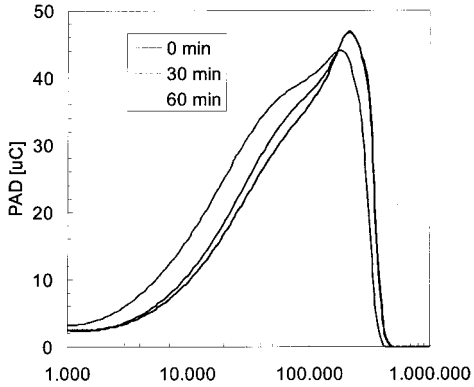

FIGURE 7: Molecular-weight distribution of xylan as a result of its degradation by the xylanase from *P. simplicissimum*.

of subsites −I to −III, with strong and specific substrate interactions, and into the section of the cleft consisting of subsites +I and +II, where substrate interactions appear to be much weaker and less specific. It is tempting and suggestive to refer to the former part of the binding cleft (subsites −I, −II, and −III) as a "substrate recognition area" and to the latter part (sites +I and +II) as a "product release area".

Xylose subunits are held in position by a sophisticated H-bonding network as well as by hydrophobic contacts with aromatic side chains of tryptophanes or tyrosines, as shown schematically in Figure 5a for the xylose rings observed in the xylotetraose experiment. There are both hydrogen bonding and stacking interactions with xylose rings bound to the subsites of the substrate recognition area, but only one stacking interaction (to Tyr175) with rings attached to the product release area. Tyr175 thus forms a rather unspecific "greasy patch." Without the possibility for the formation of specific hydrogen bonds (Figures 5b and 6a), the product release area presumably acts like a slide to release the product after hydrolysis. Accordingly, the electron density for rings bound to subsites −I to −III was always observed to be much better defined than for subsites +I and +II, where density is invariably diffuse, permitting a determination of the rough location of a xylan subunit, but no detailed assessment of orientation or conformation. Also, while subsites of the substrate recognition area were found to be occupied in all diffusion experiments, only in experiments of X1, X4, and X5 was density observed in the subsites of the product release area. In all experiments except the one with monomeric xylose, the xylooligomer attached to the substrate recognition area was found to be hydrogen bonded with its reducing end to the proton donor Glu132 side chain, and the xylotrioses observed in this area in the X3, X4, and X5 experiments were found in very similar locations and conformations.

Enzyme Kinetic Data. The above observations from the soaking experiments can best be interpreted in the light of kinetic data. The mode of action of the *P. simplicissimum* xylanase has been investigated recently (*18*), and a rapid decrease in the viscosity of a xylan preparation upon incubation with the *P. simplicissimum* xylanase was observed. In that respect, this xylanase outperformed a variety of related enzymes. Figure 7 shows the xylan molecular-weight distribution after 0, 30, and 60 min of treatment with the *P. simplicissimum* xylanase. The observed rapid broadening of the distribution indicates a distinct endo-specificity

Table 2: Michaelis−Menten Parameters for the Degradation of Xylooligosaccharides by the *Penicillium Simplicissimum* Xylanase

substrate	K_m (mM)	k_{cat} (s^{-1})	k_{cat}/K_m
X2	no reaction	no reaction	no reaction
X3	7.9	0.006	0.000 76
X4	5.1	0.8	0.16
X5	3.1	8.3	2.7
X6	1.4	9.1	6.5

of the enzyme. Analysis of the products of exhaustive xylan degradation yielded a mixture of xylotriose (main component) and xylobiose (minor component) as the smallest hydrolysis products, and the minimum substrate length for cleavage was found to be xylotetraose (*18*).

We have determined enzyme kinetic data on the hydrolysis of xylooligomers by the *P. simplicissimum* xylanase with a degree of oligomerization between $n = 2$ and $n = 6$ in order to put the previous observations on a more quantitative basis. Our results are presented in Table 2: while the K_m values decrease more or less continually between $n = 3$ and $n = 6$, the k_{cat} values increase with the chain length, in agreement with data reported previously for a xylanase from *Schizophyllum commune* (*5*). This increase amounts to more than 2 orders of magnitude difference between $n = 3$ and $n = 4$, and about 1 order of magnitude from the tetraose to the pentaose, with a very small increase (at the detection limit) between X5 and X6.

For the xylotriose, the kinetic data thus indicate appreciable binding ($K_m \approx 8$ mM) but almost no catalysis ($k_{cat} \approx 0.006$). This is readily explained from the results of the soaking experiments. As observed in the X3 experiment, the triose preferentially binds to the substrate recognition area (subsites −I to −III). In order for it to be hydrolyzed, it would have to shift the xylose ring at its reducing end across the cleavage site, which is energetically unfavorable in view of the weaker binding of a ring in subsite +I of the product release area as compared to subsite −III of the substrate recognition area.

A similar explanation might then have to account for the fact that the tetraose is still 10 times less efficiently cleaved than the pentaose ($k_{cat} \approx 0.8$ vs 8.3). If an analogous reason applies as for the triose, we have to assume that binding to subsite −IV is still more efficient than to +I, which seems to contradict the evidence from the soaking experiments. However, the fact that only 3 rings were observed in the substrate recognition subsites for the X4 and X5 experiments may be due to crystal packing, with a neighboring molecule blocking the access to subsite −IV.

Thus, the observed minimum substrate length (xylotetraose) is due to the stronger binding of the first 3−4 xylane rings to the subsites of the substrate recognition area as compared to the product release area. As an obvious consequence, we expect small oligomeric hydrolysis products (X1−X3) to act as inhibitors via blocking the substrate recognition area. Binding of the reaction products to the xylanase is therefore likely to regulate the xylanase activity by feedback inhibition, keeping the amount of released reducing sugars below a certain level.

One of the referees suggested an alternative interpretation of the observed structural and kinetic results: accordingly, the substrate undergoes distortion at the active site during catalysis (*10*, *33*), which occurs presumably at the expense of ligand affinity. Ligation of subsites −I and −II by X3

may provide inadequate free energy to permit the distortion at site +I, suggesting that a ligand must occupy subsites −I, −II, and −III in order to provide sufficient free energy for distortions of the xylose subunit at subsite +I. X5 is then hydrolyzed 10 times faster than ×4 simply because the enzyme stabilizes an X5 transition state more effectively than an X4 transition state. This may be due to the additional mechanical leverage the enzyme may have in using both subsites +I and +II to cause distortions in the substrate at the cleavage site. However, with the available structural and kinetc data, we see no way to distinguish between the two interpretations.

In any case, the crystallographic data suggest that subsites −I and −II are the binding sites with the highest affinity. Since the xylanase's substrate specificity [involving pronounced discrimination between, e.g. cellulose and xylane (*30*)] is most probably due to differential binding of different polymeric glycosides, the specificity has to originate primarily from the first two or three subsites of the substrate recognition area.

Branched Oligomers. The presence of "branches" in the oligosaccharide chain obviously does not prevent its binding to the substrate recognition area, as indicated by the density observed in the HexAX3-experiment. Compared to the other complexes, the subunit in subsite −III appeares to be rotated by 180° around the bond between C1 and the glycosidic oxygen. Notably, the electron density of the subunit in site −I was found to be lower than the corresponding density in the X2−X5 maps (Figure 2b). Our tentative interpretation of this observation also reflects back on the affinity of the *P. simplicissimum* xylanase toward branched substrates: there is chromatographic evidence for an impurity in the compound HexAX3 by the analogous xylobiose-derivative HexAX2 (see Figure 1), which would then compete for the xylose binding sites. We assume that the branching, although not crystallographically visible, prevents the dimeric HexAX2 from entering far enough "up" the cleft to occupy the subsites −I and −II (like X2) with its main-chain xylose units, which therefore has to put up with sites −II and −III. The observable density would then be due to the superposition of HexAX3 molecules in subsites −I to −III and HexAX2 molecules in subsites −II and −III, as illustrated in Figure 4, explaining the lower density observed in site −I. Provided the above interpretation is correct, its implications for predicting the behavior of the *P. simplicissimum* xylanase toward branched substrates is quite straightforward: accordingly, branches are tolerated at the position of subsite −III, where the active-site cleft starts to widen. No branches would then be tolerated at subsites −I and −II, where the cleft is narrower and deeper. The *P. simplicissimum* xylanase is likely to degrade branched xylan chains, as long as it finds an unbranched segment of more than two monomers "upstream" (i.e., toward the reducing end) from the branched xylose ring.

Bound Substrate Molecules in Other Xylanase Crystal Structures. Two other crystal structures of family 10 xylanases with bound substrates or substrate analogues have been reported so far. One is the structure of the E246C mutant of the *Pseudomonas fluorescens* subspecies *cellulosa* xylanase A complexed with xylopentaose (*19*), for which no 3D coordinates are available, the other one is the xylanase Cex from *Cellulomonas fimi*, with 2-deoxy-2-fluoro cellobioside (2D2FC) covalently attached to the nucleophile Glu233 (*40*). A superposition of the sugar subunit positions between the xylotriose (X3) complex of *P. simplicissimum* and the above *C. fimi* xylanase complexed with 2D2FC is shown in Figure 6c: while the xylose rings attached to subsite −II agree very well between the two structures, the ring in subsite −I is pulled deeper into the catalytic center of the *C. fimi* enzyme as a result of a covalent bond between the anomeric carbon C1 and the carboxyl oxygen OE1 of Glu233. The *C. fimi* complex has been designed to constitute a model for the reaction intermediate following removal of the reducing end of the xylan chain, but before hydrolysis of the enzyme−xylan complex, as expected for a retaining glycosyl hydrolase (*10*). In the *P. simplicissimum* structure, the xylose subunit in site −I is not covalently attached but with its O2 in hydrogen-bonding contact to the nucleophile (Glu238) and forms a hydrogen bond with the putative proton donor Glu132. Such an interaction is not observed in the 2-deoxy-2-fluoro complex of *C. fimi*. What we see in the *P. simplicissimum* complex crystal structure can be interpreted as the situation following hydrolysis of the covalent intermediate, with all reactants fully recovered.

Implications for Enzyme Catalysis. Under conditions of very high substrate saturation, the state of an enzyme will depend on the relative rates of catalysis versus product release. If the former is rate limiting, one expects the protein to occur predominantly in a Boltzmann-like distribution of states preceding the rate-limiting catalysis step. If product release is rate limiting, the Boltzmann distribution will include *all* states along the reaction coordinate.

Crystallographically, one observes binding of xylooligomers X*n* to the "substrate recognition area" up to $n = 3$. For $n = 4$ and $n = 5$, two fragments of the oligomer are observed, a xylotriose at the "substrate recognition area", and a monomer or dimer in the "leaving-group area". These observations can be interpreted, at least qualitatively, to indicate that, *under the conditions prevailing within the enzyme crystal*, the latter situation—release of hydrolysis products being rate limiting—applies to the experiments with xylotetraose and xylopentaose, while for the two shorter xylooligomers, catalysis appears to be rate limiting.

The observations from the soaking experiments with xylotetraose X4 and xylopentaose X5 can thus be interpreted as corresponding to the Michaelis−Menten complex of the reverse reaction, i.e., the enzyme-catalyzed condensation of a trimer plus a monomer or dimer to form a tetra- or pentamer. It is well-known that xylanases, when supplied with high amounts of short xylooligomers, are capable of resynthesizing larger oligomers (*2*, *3*).

Secondary Xylose Binding Site. An additional binding site for one single xylose molecule was observed on the opposite side of the enzyme molecule (see Figure 5b). A functional significance for this binding site is not evident from the crystal structures. Since a direct involvement in substrate binding or catalysis of a xylose molecule attached to this binding site is unlikely due to the large distance to the active site, we performed differential scanning calorimetry experiments in the presence and absence of xylose to investigate the possibility that binding of xylose might enhance protein stability. However, no stabilizing effect of xylose (data not shown) could be detected. The presence of a secondary, noncatalytic, xylan specific binding site is not unprecedented

(*4*), and it remains to be shown whether binding of xylose to this secondary site has a functional significance by influencing the protein's mobility.

MATERIALS AND METHODS

Crystallization and Xylooligosaccharide Preparation. The xylanase from *Penicillium simplicissimum* was crystallized as described previously (*32*). Xylooligosaccharide substrates (which are referred to as X2, X3 X4, X5, and X6 for β-D-xylobiose, xylotriose, xylotetraose, xylopentaose, and xylohexaose, respectively, see Figure 1) were produced from birchwood xylan (Roth, Karlsruhe, Germany). The xylan was partially hydrolyzed with the xylanase from *Thermomyces lanuginosus* (*31*) and the reaction products were filtrated and concentrated by freeze-drying. The sample was then applied to a charcoal/Celite column (1:1, v/v) and eluted stepwise with increasing ethanol concentration (water:ethanol from 1:0 up to 4:1). The monomer (X1) D-xylose was purchased from Fluka. The branched compound HexAX3 was kindly supplied by Dr. M. Tenkanen, VTT Biotechnology and Food Research, Espoo, Finnland.

Enzyme Kinetics. Xylose and xylooligosccharides (standards from Seikagaku) were quantified by HPLC using a CarboPac PA-1 column from Dionex as described previously (*42*). For the hydrolysis experiments, solutions of 0.5% (w/v) wheat arabinoxylan (Megazyme) and of xylooligomers with concentrations ranging from 0.1 to 8 mM in 50 mM sodium-citrate buffer (pH 6.0) were incubated with about 0.1 units/ml of the *P. simplicissimum* xylanase at 30 °C. The K_m and k_{cat} values of the xylanase based on the amount (nmol) of oligomer degraded per second as initial reaction rate were determined by nonlinear analysis using the program SigmaPlot version 3.02. The molecular weight of partially hydrolyzed arabinoxylan (see Figure 7) was determined by HPLC using Toyopearl HW-55S and HW-50S columns as described previously (*42*). Elution of the samples was monitored using an electrochemical PAD (Pulsed Amperometric Detector). Xylooligosaccharides from DP2−6 (Megazyme) and dextrans (T10, T40, T70, and T500 from Pharmacia) were used as standards.

Preparation of Xylooligosaccharide Solutions. Water was pretreated using a MilliQ system. Chemicals were purchased from Sigma and Fluka. The xylooligosaccharides (in the form of a lyophilized powder obtained from the above preparation) were dissolved in a liquid containing 60% v/v reservoir solution from the crystallization and 40% v/v water to give a concentration of 20% w/v. In the case of the less-soluble xylobiose, a saturated solution instead of 20% w/v was used. Solutions were tested with respect to their capability to function as a cryoprotectant: a drop of the solution was frozen by dumping into liquid nitrogen, and the solution was deemed acceptable when the frozen drop remained clear. Since the xylooligomers alone were not sufficient in this test, a small amount of 2-methyl-2,4-pentanediole (MPD) was added. The final cryoprotectant solution thus typically consisted of 90 or 95% v/v xylooligomer-solution and 10 or 5% MPD.

For the native PEG200 dataset, the cryoprotectant solution consisted of 20% v/v poly(ethylene glycol) (PEG-200) and 80% reservoir solution.

Soaking Experiment. Native enzyme crystals were soaked in the corresponding xylooligosaccharide/MPD solutions at 4 °C, with the exception of X2, for which the experiment was carried out at room temperature. Using a nylon fiber cryo-loop (Hampton) attached to a pointed aluminum pin, the crystal was transferred into a 5−10 μL drop containing the cryoprotectant and was left there for about 30 s. It was then picked up with the same loop, dumped into liquid nitrogen, and subsequently mounted on the X-ray goniometer for data collection. The same procedure was used for the native PEG200 crystal.

Data Collection and Processing. The data were collected at a temperature of 100−110 K (locally constructed cold-stream device) on a Siemens rotating-anode X-ray generator ($\lambda = 1.54$ Å) equipped with a MARresearch goniometer with imaging plate detector. The PEG200 dataset was collected at the EMBL-beamline X11 ($\lambda = 0.9058$ Å) at DESY in Hamburg, Germany. This beamline was equipped with a cryostream-cooling device and a MAR imaging-plate scanner. Data were processed using programs DENZO and SCALEPACK (*29*) and the routine TRUNCATE of the CCP4 suite (*1*).

Refinement. The complex structures were refined with the program X-PLOR (*7, 8*), starting with a rigid body refinement of the native molecule against complex data. After positional refinement, electron density maps ($2F_o - F_c$ and $F_o - F_c$) were computed, side-chains conformations were adjusted, and water and substrate molecules were fitted into the residual electron density, using the graphical program O (*25*). The coordinates for a single D-xylose molecule were obtained from the Heterocompound Information Centre Uppsala (HICup, http://alpha2.bmc.uu.se/hicup/), parameter and topology files as required by X-PLOR for the xylooligomers were set up using the existing carbohydrate related files as templates. To avoid overfitting, 10% of the data were set aside for monitoring R_{free} (*6*). Individual *B*-factors were only refined when justified by the maximum resolution of the data, i.e., when the data extended to beyond 2.2 Å. Following crystallographic refinement, each structure was validated with the program Procheck (*27*). In all cases, more than 90% of non-Pro and non-Gly residues were observed in most favored regions of the Ramachandran plot, and none in forbidden regions. RMS deviations from ideal bonding geometries were insignificant.

ACKNOWLEDGMENT

The PEG200 dataset was collected at the EMBL-beamline X11 at DESY in Hamburg, Germany. We acknowledge help from Victor Lamzin in collecting these data. The branched xylooligomer HexAX3 was generously supplied by Dr. M. Tenkanen (VTT Biotechnology and Food Research, Espoo, Finland), and raw extract of *P. simplicissimum* xylanase by W. Steiner, both of which is gratefully acknowledged. We thank one of the referees for suggesting an alternative mechanistic interpretation for the observed kinetic and structural results on the *P. simplicissimum* xylanase.

REFERENCES

1. Bailey, S. (1994) *Acta Crystallogr., Sect. D 50*, 760−763.
2. Biely, P., and Vrsanska, M. (1983) *Eur. J. Biochem. 129*, 645−51.
3. Biely, P., Vrsánská, M., and Krátký, Z. (1981) *Eur. J. Biochem. 119*, 565.

4. Black, G. W., Hazlewood, G. P., Millward Sadler, S. J., Laurie, J. I., and Gilbert, H. J. (1995) *Biochem. J. 307*, 191−5.
5. Bray, M. R., and Clarke, A. J. (1992) *Eur. J. Biochem. 204*, 191−196.
6. Brunger, A. T. (1992) *Nature 355*, 472−474.
7. Brunger, A. T. (1992) X-PLOR, a System for X-ray Crystallography and NMR, Version 3.2, Yale University Press, New Haven, Ct.
8. Brunger, A. T., Kuriyan, J., and Karplus, M. (1987) *Science 235*, 458−460.
9. Campbell, R. L., Rose, D. R., Wakarchuk, W. W., To, R., Sung, W., and Yaguchi, M. (1992) in *Trichoderma reesei Cellulases and Other Hydrolases* (Suominen, P., and Reinikainen, T., Eds.) pp 63−72, Foundation for Biotechnical and Industrial Fermentation Research.
10. Davies, G., and Henrissat, B. (1995) *Structure 3*, 853−859.
11. Davies, G., Sinnott, M. L., and Withers, S. G. (1998) in *Comprehensive Biological Catalysis* (Sinnott, M., Ed.) pp 119−209, Academic Press, London.
12. Davies, G. J., Wilson, K. S., and Henrissat, B. (1997) *Biochem. J. 321*, 557−559.
13. Derewenda, U., Swenson, L., Green, R., Wei, Y. Y., Morosoli, R., Shareck, F., Kluepfel, D., and Derewenda, Z. S. (1994) *J. Biol. Chem. 269*, 20811−20814.
14. Dominguez, R., Souchon, H., Spinelli, S., Dauter, Z., Wilson, K. S., Chauvaux, S., Beguin, P., and Alzari, P. M. (1995) *Nat. Struct. Biol. 2*, 569−576.
15. Garman, E. F., and Schneider, T. R. (1997) *J. Appl. Crystallogr. 30*, 211−237.
16. Gilkes, N. R., Claeyssens, M., Aebersold, R., Henrissat, B., Meinke, A., Morrison, H. D., Kilburn, D. G., Warren, R. A. J., and Miller, R. C. (1991) *Eur. J. Biochem. 202*, 367−377.
17. Gruber, K., Klintschar, G., Hayn, M., Schlacher, A., Steiner, W., and Kratky, C. (1998) *Biochemistry 37*, 13475−13485.
18. Gübitz, G. M., Haltrich, D., Latal, B., and Steiner, W. (1997) *Appl. Microbiol. Biotechnol. 47*, 658−662.
19. Harris, G. W., Jenkins, J. A., Connerton, I., Cummings, N., Loleggio, L., Scott, M., Hazlewood, G. P., Laurie, J. I., Gilbert, H. J., and Pickersgill, R. W. (1994) *Structure 2*, 1107−1116.
20. Harris, G. W., Jenkins, J. A., Connerton, I., and Pickersgill, R. W. (1996) *Acta Crystallogr., Sect. D 52*, 393−401.
21. Harris, G. W., Pickersgill, R. W., Connerton, I., Debeire, P., Touzel, J. P., Breton, C., and Perez, S. (1997) *Proteins 29*, 77−86.
22. Havukainen, R., Törrönen, A., Laitinen, T., and Rouvinen, J. (1996) *Biochemistry 35*, 9617−9624.
23. Henrissat, B. (1991) *Biochem. J. 280*, 309−316.
24. Henrissat, B., and Bairoch, A. (1993) *Biochem. J. 293*, 781−788.
25. Jones, T. A., Zou, J. Y., Cowan, S., and Kjeldgaard, M. (1991) *Acta Crystallogr., Sect. A 47*, 110−119.
26. Kraulis, P. J. (1991) *J. Appl. Crystallogr. 24*, 946−950.
27. Laskowski, R. A., MacArthur, M. W., Moss, D. S., and Thornton, J. M. (1993) *J. Appl. Crystallogr. 26*, 283−291.
28. Nicholls, A. J. (1993) GRASP: Graphical Representation and Analysis of Surface Properties, Columbia University, New York.
29. Otwinowsky, Z. (1993) in *Data collection and processing* (Sawyer, L., Isaacs, N., and Bailey, S., Eds.) pp 55−62, Daresbury Laboratory, Warrington WA4 4AD, England.
30. Schall, S. (1994) Ph.D. Thesis, Formal und naturwissenschaftliche Fakultät, Universität Wien, Wien.
31. Schlacher, A., Holzmann, K., Hayn, M., Steiner, W., and Schwab, H. (1996) *J. Biotechnol. 49*, 211−218.
32. Schmidt, A., Schlacher, A., Steiner, W., Schwab, H., and Kratky, C. (1998) *Protein Sci. 7*, 2081−2088.
33. Sinnot, M. L. (1990) *Chem. Rev. 90*, 1171−1202.
34. Sulzenbacher, G., Driguez, H., Henrissat, B., Schulein, M., and Davies, G. J. (1996) *Biochemistry 35*, 15280−15287.
35. Sulzenbacher, G., Schulein, M., and Davies, G. J. (1997) *Biochemistry 36*, 5902−5911.
36. Teleman, A., Harjunpaa, V., Tenkanen, M., Buchert, J., Hausalo, T., Drakenberg, T., and Vuorinen, T. (1995) *Carbohydr. Res. 272*, 55−71.
37. Törrönen, A., Harkki, A., and Rouvinen, J. (1994) *EMBO J. 13* (11), 2493−2501.
38. Törrönen, A., and Rouvinen, J. (1995) *Biochemistry 34*, 847−856.
39. Tull, D., and Withers, S. G. (1994) *Biochemistry, 33*, 6363−6370.
40. White, A., Tull, D., Johns, K., Withers, S. G., and Rose, D. R. (1996) *Nat. Struct. Biol. 3*, 149−154.
41. White, A., Withers, S. G., Gilkes, N. R., and Rose, D. R. (1994) *Biochemistry 33*, 12546−12552.
42. Wong, K. Y., Yotoya, S., Saddler, J. N., and deJong, E. (1996) *J. Wood Sci. Technol. 16*, 121−138.

BI982108L